Electronic Supporting Information for the manuscript (ESI):

Deoxydehydration of glycerol in presence of rhenium compounds: reactivity and mechanistic aspects

Massimiliano Lupacchini,[a] Andrea Mascitti,[a] Valentino Canale,[b] Lucia Tonucci,[c] Evelina Colacino,[d] Maurizio Passacantando,[e] Alessandro Marrone[c*] and Nicola d'Alessandro[a*]

[a] Department of Engineering and Geology, University G. d'Annunzio of Chieti-Pescara, Via dei Vestini 31, 66100, Chieti Scalo, Italy
E-mail: nicola.dalessandro@unich.it

[b] Department of Pharmacy, University G. d'Annunzio of Chieti-Pescara, Via dei Vestini 31, 66100, Chieti Scalo, Italy
E-mail: amarrone@unich.it

[c] Department of Philosophical, Educational and Economic Sciences, University G. d'Annunzio of Chieti-Pescara, Via dei Vestini 31, 66100, Chieti Scalo, Italy

[d] Institut Charles Gerhardt de Montpellier (ICGM), UMR-5253 CNRS-UM-ENSCM, c/o Ecole Nationale Supérieure de Chimie de Montpellier, 8 Rue de l'Ecole Normale, 34296, Montpellier Cedex 05 (France).

[e] Department of Physical and Chemical Sciences, University of L'Aquila, Via Vetoio, I-67100 L'Aquila, Italy

* Corresponding authors: nicola.dalessandro@unich.it and amarrone@unich.it

Supporting Information Captions

Figure S1. Schematic apparatus used to carry out the Re catalysed DODH reaction on glycerol

Figure S2. A typical NMR spectrum of allyl alcohol recorded from the water trap by any DODH experiment. Spectra were acquired in water suppression mode. Allyl alcohol signals are recorded at 4.05, 5.15 and 5.95 ppm. The remaining signals are attributed to vaporization of DMP (and its oxidation derivative).

Figure S3. FT-IR spectrum of MTO (**1**).

Figure S4. FT-IR spectrum of MTO (**1**) after the delay time.

Figure S5. FT-IR spectrum of ReO_3 (**2**) after the delay time.

Figure S6. FT-IR spectrum of $ReCl_5$ (**4**)

Figure S7. FT-IR spectrum of $ReCl_5$ (**4**) after the delay time.

Figure S8. FT-IR spectrum of Re_2O_7 (**5**)

Figure S9. FT-IR spectrum of Re_2O_7 (**5**) after the delay time.

Figure S10. FT-IR spectrum of ReI_3 (**7**)

Figure S11. FT-IR spectrum of ReI_3 (**7**) after the delay time.

Figure S12. FT-IR spectrum of $ReO_2I[P(C_6H_5)_3]_2$ (**11**)

Figure S13. FT-IR spectrum of $ReO_2I[P(C_6H_5)_3]_2$ (**11**) after the delay time.

Figure S14. The mass spectrum of monodeuterated methane recorded by sampling the headspace of the reaction medium containing monodeuterated DMP (-OD) and MTO, and after a time comprised in the range of the detected delay time (MTO + DMP at 140 °C).

Figure S15. GC-MS profile of water trap headspace recorded after 10 min from the addition of glycerol. The catalyst (MTO) used in the present experiment was pretreated at 140C° in presence of only DMP for the delay time previously established (45 min). It is worth noting the almost immediate appearance of the chromatographic peak of allyl alcohol.

Figure S16. X-ray diffraction (XRD) of **1**, on samples treated at 140 °C and 450 °C.

Figure S17. Ball-and-sticks representations of the calculated transition state structures for the methane release process (left) and MTO reduction (right).

Figure S18. Ball-and-sticks representation of the optimized structure of $[ReO_3(2\text{-PrO})\cdot 2\text{-PrOH}]_2$ (right) and $[ReO_2(2\text{-PrO})\cdot 2\text{-PrOH}]_2$ (left). For sake of clarity, non-polar hydrogen are not displayed. Dashed lines indicate Re-Re distance (black) and hydrogen bond contacts (green). Bond distances in Angstrom.

Figure S19. Comparison between the experimental IR spectra of MTO and Re_2O_7 precipitate after the delay time and the theoretical IR spectra of $[ReO_3(2PrO)\cdot 2PrOH]_2$ and $[ReO_2(2\text{-PrO})\cdot 2\text{-PrOH}]_2$.

Figure S20. GC-MS chromatogram recorded during the course of DODH in presence of ReO_3, in neat glycerol. Note that the chromatographic response factors of the various by-products like acrolein, allyl formate, diallyl ester, and allyl acetate are noticeably higher than that of allyl alcohol.

Scheme S1. Hypothesized solvent-assisted processes affording methane from MTO: A) two-step, and B) one-step (concerted) mechanism.

Table S1. Comparison between the experimental IR spectra of **1** and **5** after delay time and the theoretical IR spectra of $[ReO_3(2\text{-}PrO)\cdot PrOH]_2$ and $[ReO_2(2\text{-}PrO)\cdot PrOH]_2$ in the gas phase.

Table S2. % Yields of acrolein in reactions conducted under air and hydrogen at 140 °C, in DMP; the reaction was stopped when allyl alcohol finished to be formed.

Table S3: Oxygen to rhenium ratio, determined gravimetrically, simply recovering the residue of each Re compound, after 8 hours of treatment at 140 °C, and subsequently after a treatment at 450 °C

Table S4. Rhenium content by ICP AES of samples recovered after a treatment of 8 hours at 140 °C

Table S5. Cartesian coordinates (in Angstrom) of transition state structures.

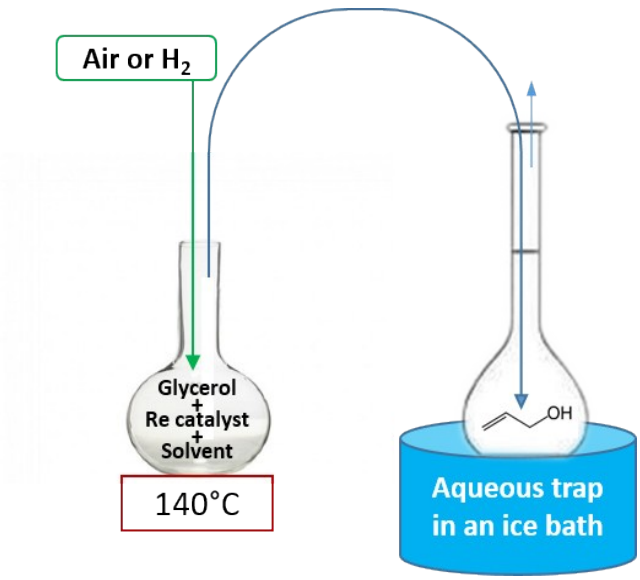

Figure S1. Schematic apparatus used to carry out the Re catalysed DODH reaction on glycerol

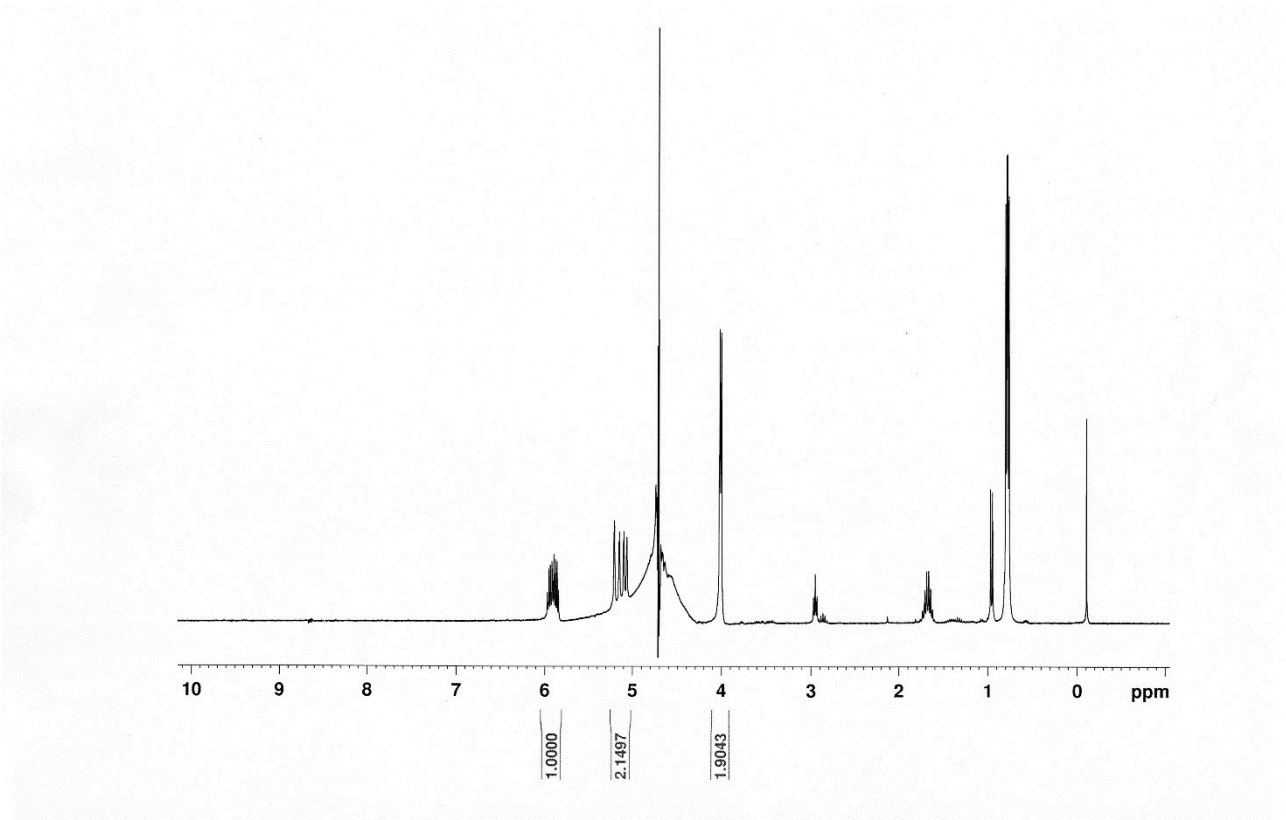

Figure S2. A typical NMR spectrum of allyl alcohol recorded from the water trap by any DODH experiment. Spectra were acquired in water suppression mode. Allyl alcohol signals are recorded at 4.05, 5.15 and 5.95 ppm. The remaining signals are attributed to vaporization of DMP (and its oxidation derivative).

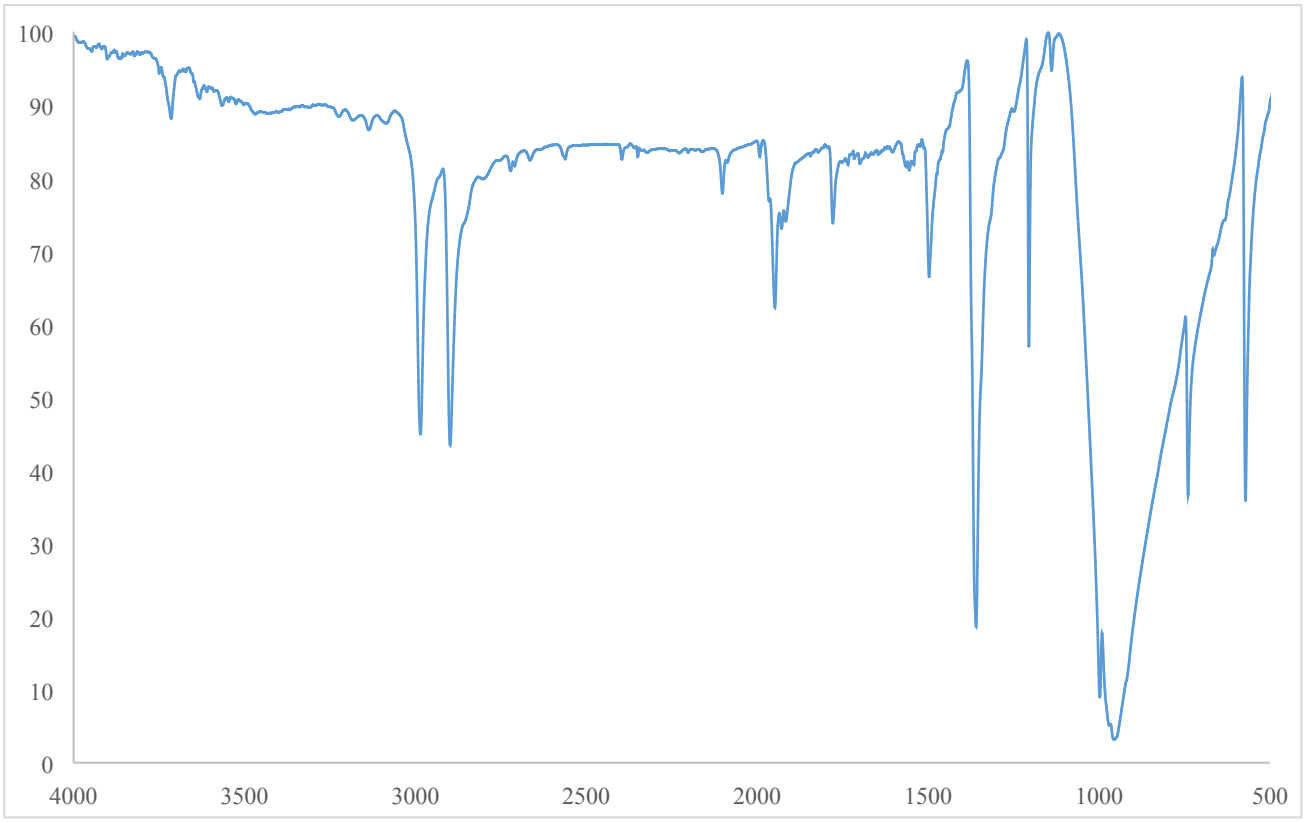

Figure S3. FT-IR spectrum of MTO (**1**).

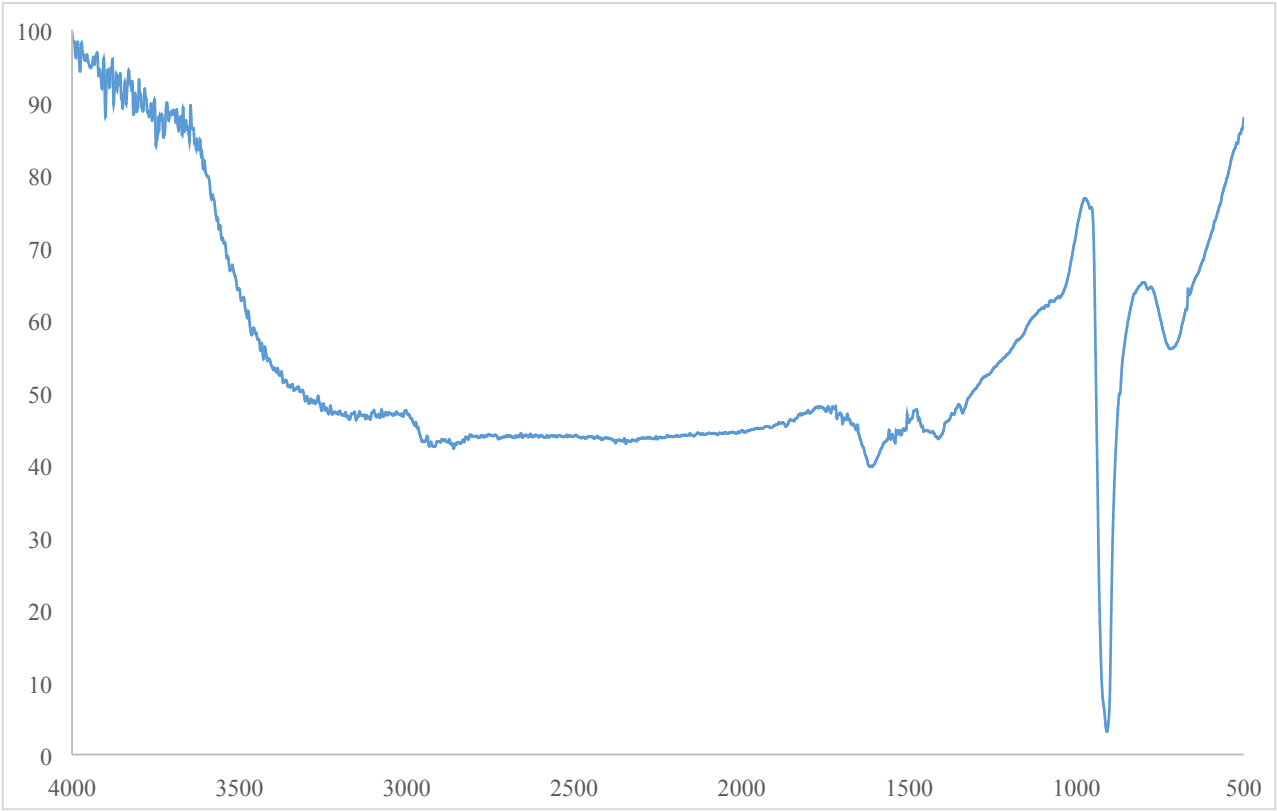

Figure S4. FT-IR spectrum of MTO (**1**) after the delay time.

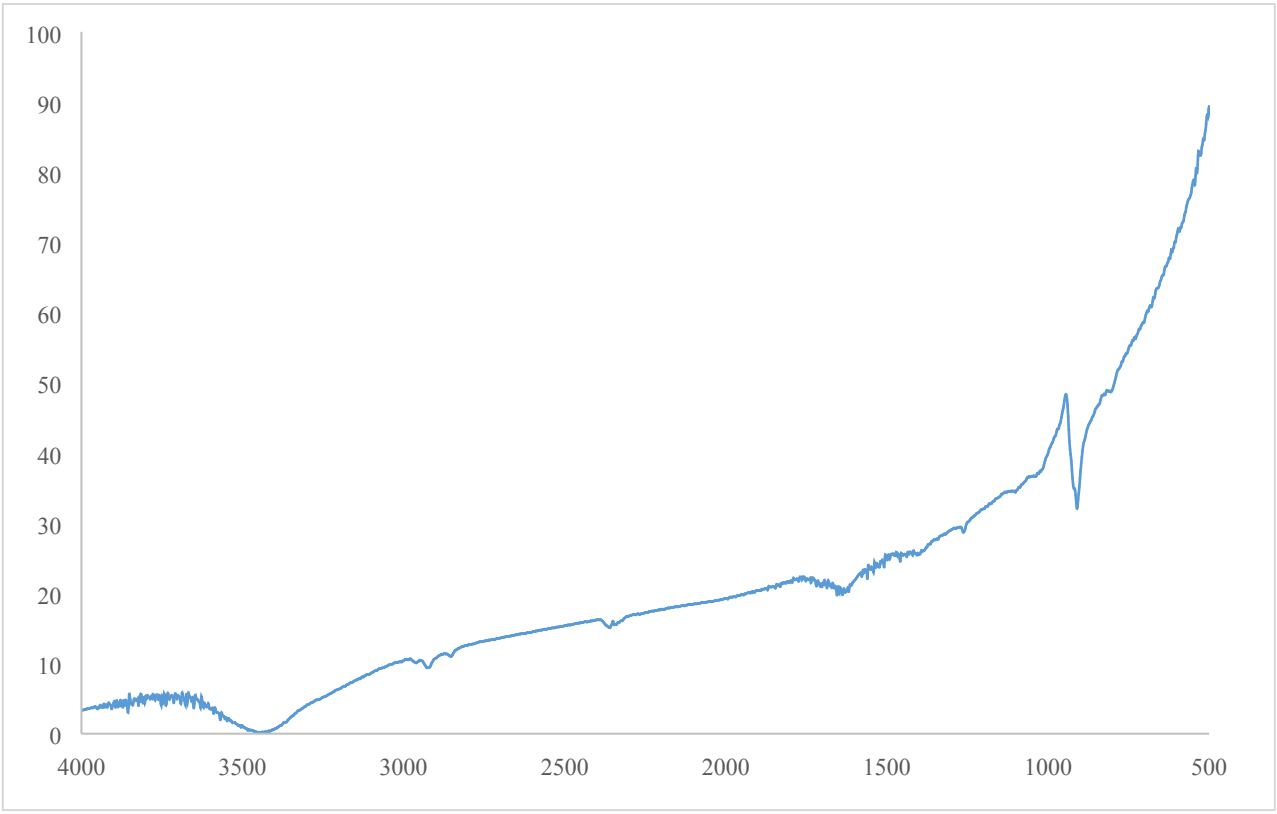

Figure S5. FT-IR spectrum of ReO_3 (**2**) after the delay time.

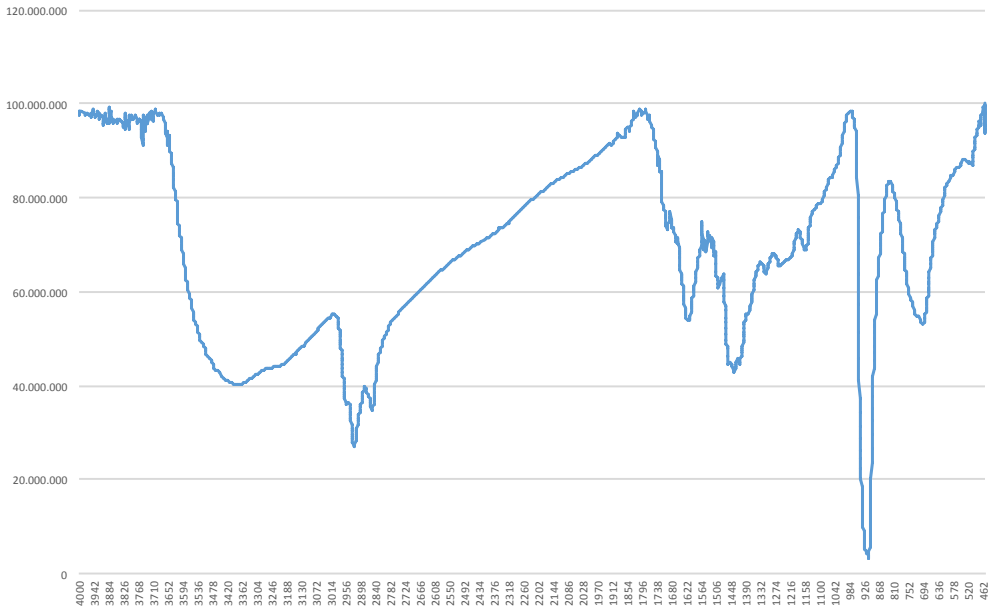

Figure S6. FT-IR spectrum of $ReCl_5$ (**4**)

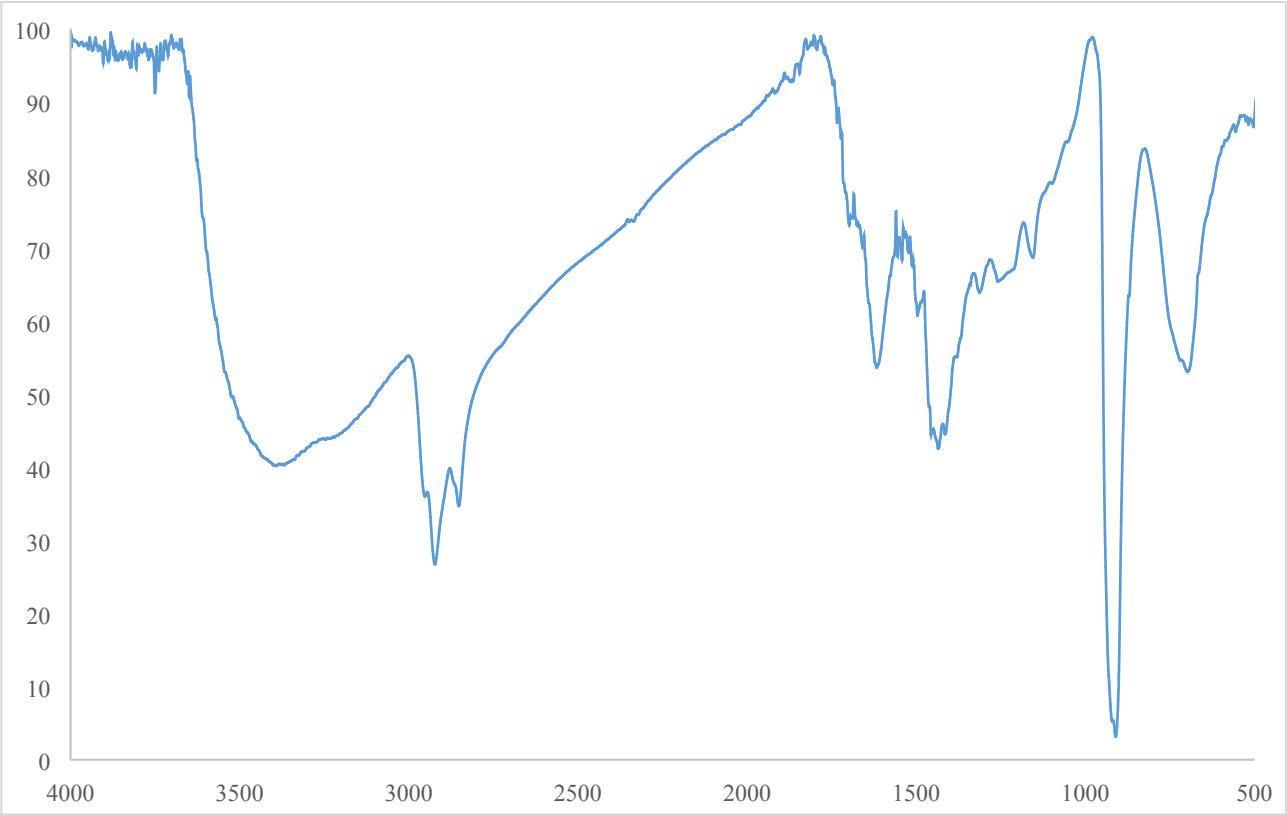

Figure S7. FT-IR spectrum of $ReCl_5$ (**4**) after the delay time.

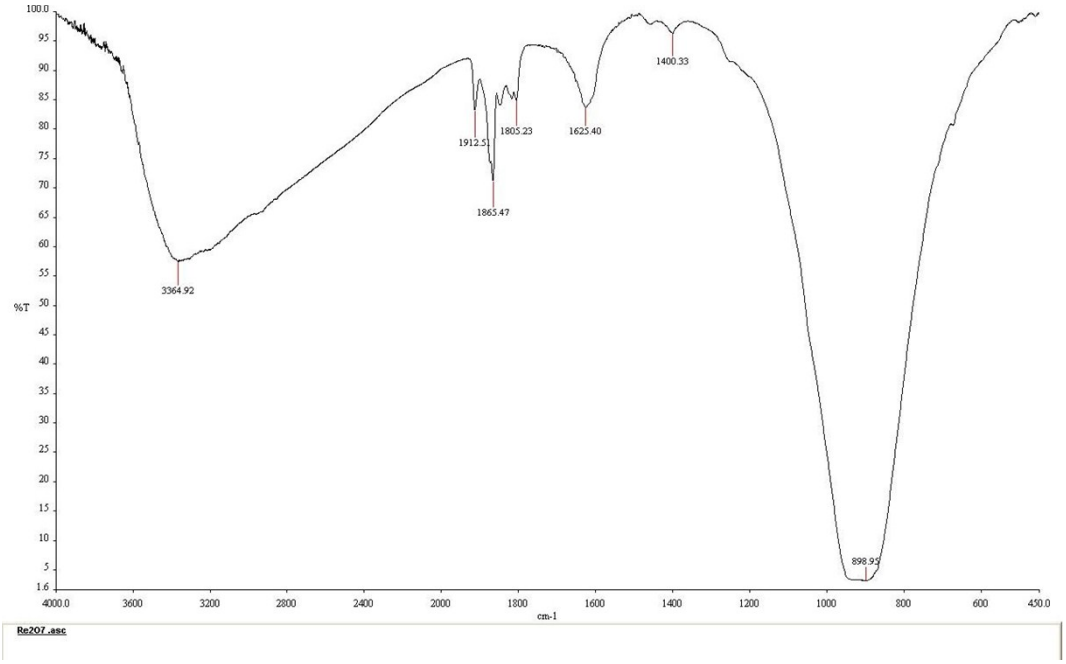

Figure S8. FT-IR spectrum of Re_2O_7 (**5**)

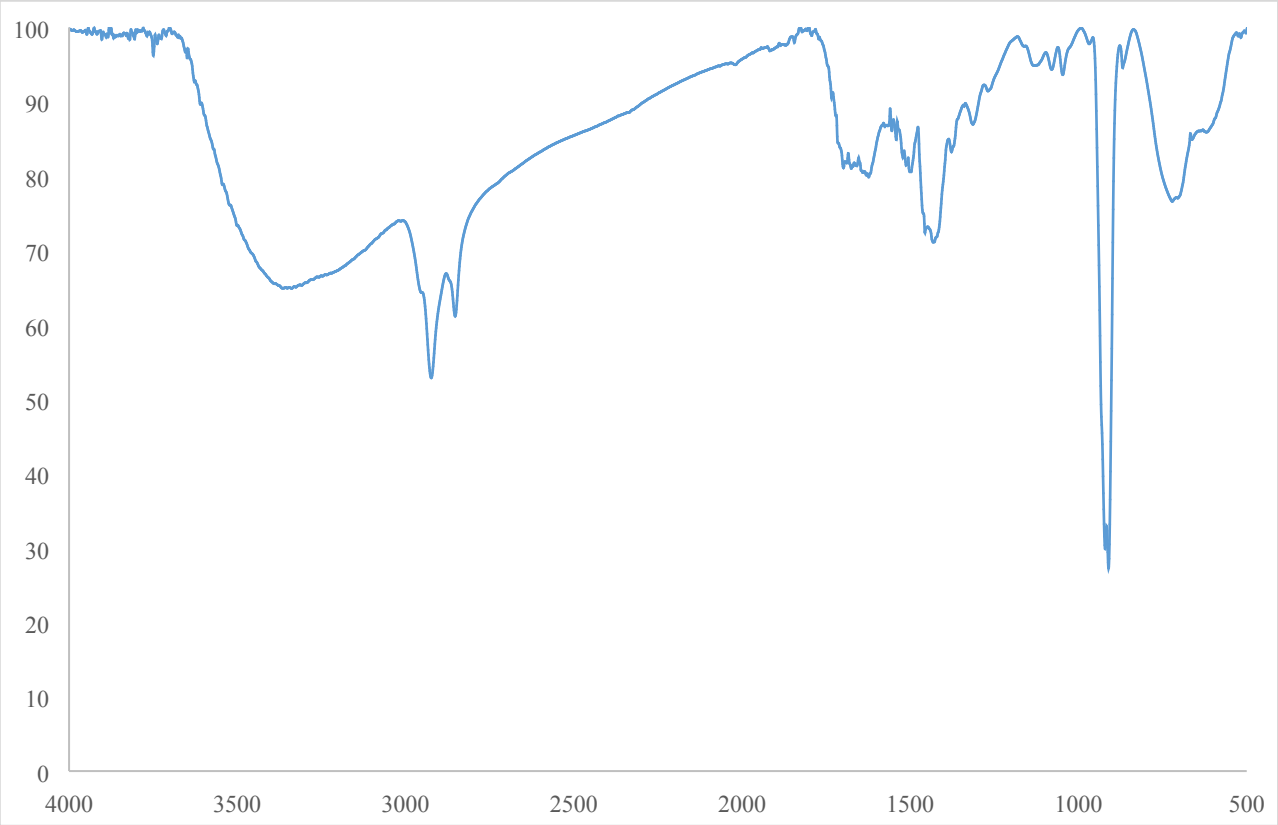

Figure S9. FT-IR spectrum of Re_2O_7 (**5**) after the delay time.

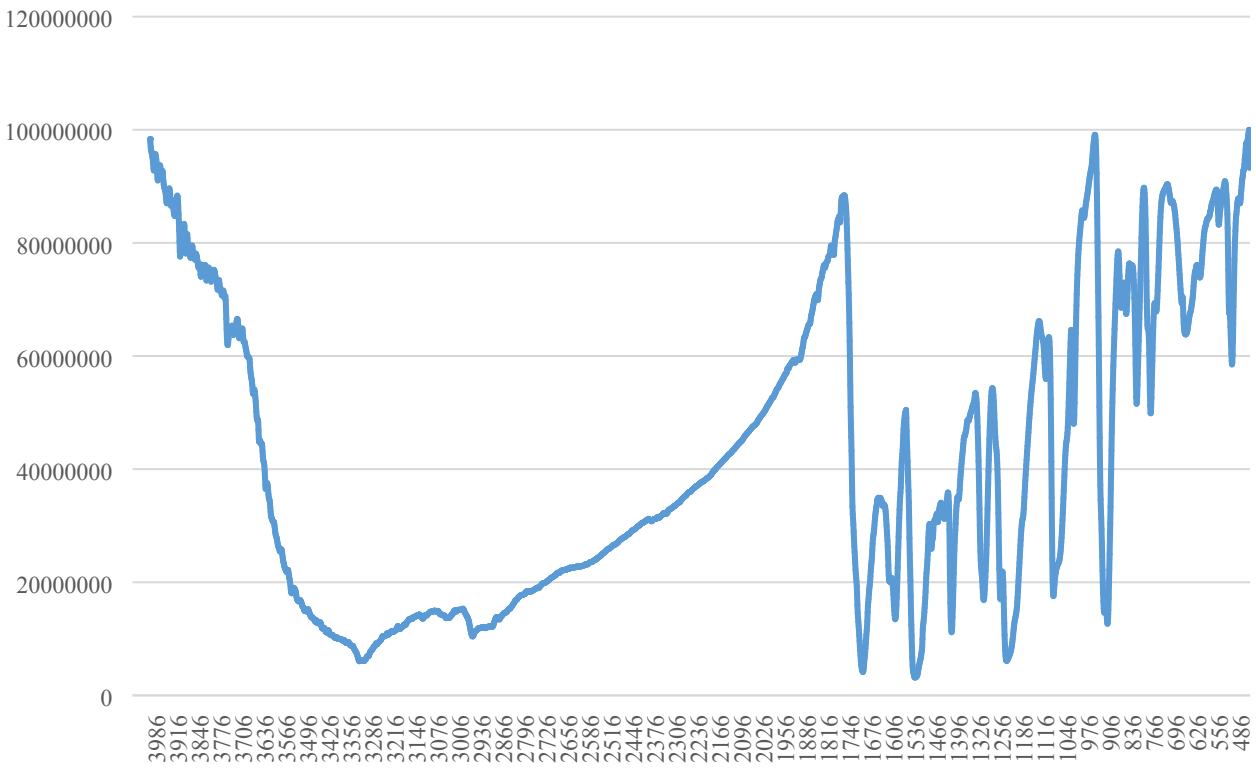

Figure S10. FT-IR spectrum of ReI_3 (**7**)

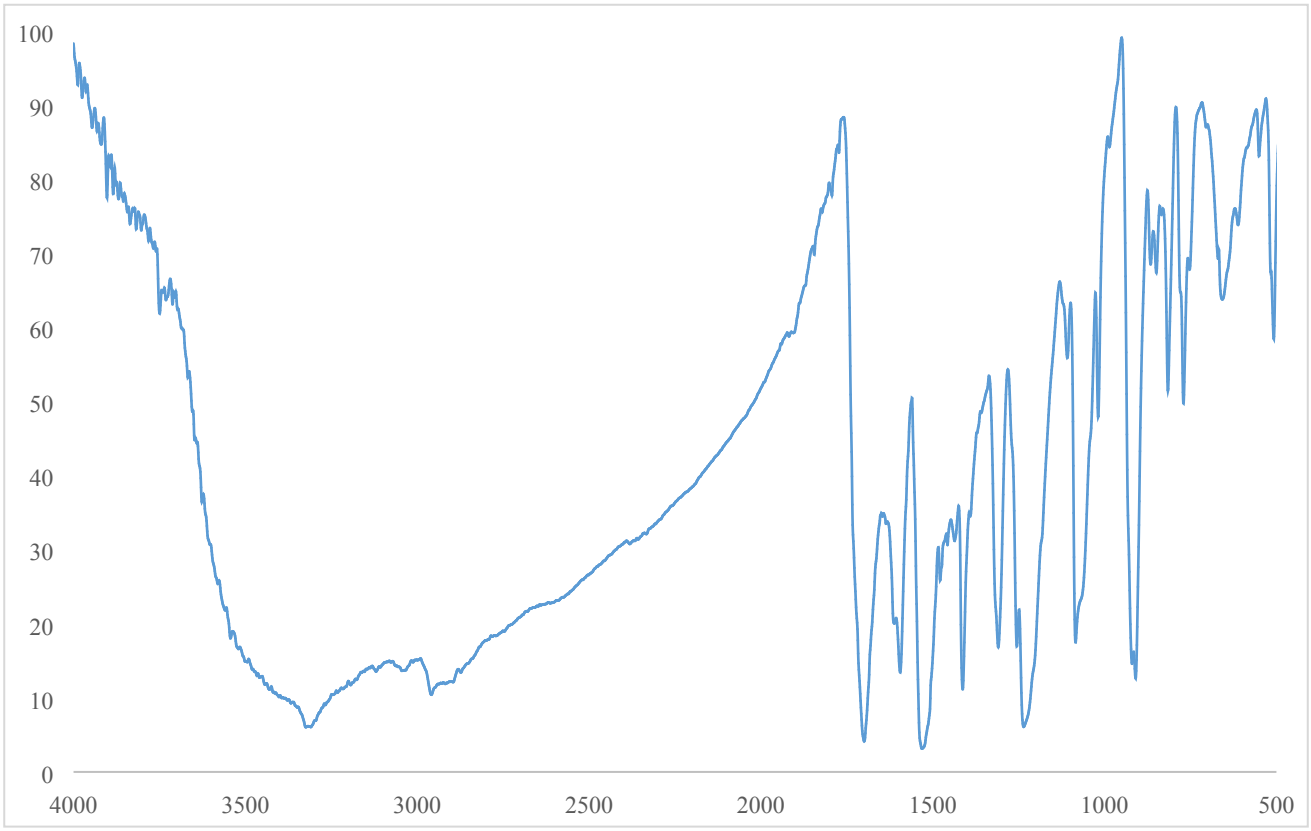

Figure S11. FT-IR spectrum of ReI_3 (**7**) after the delay time.

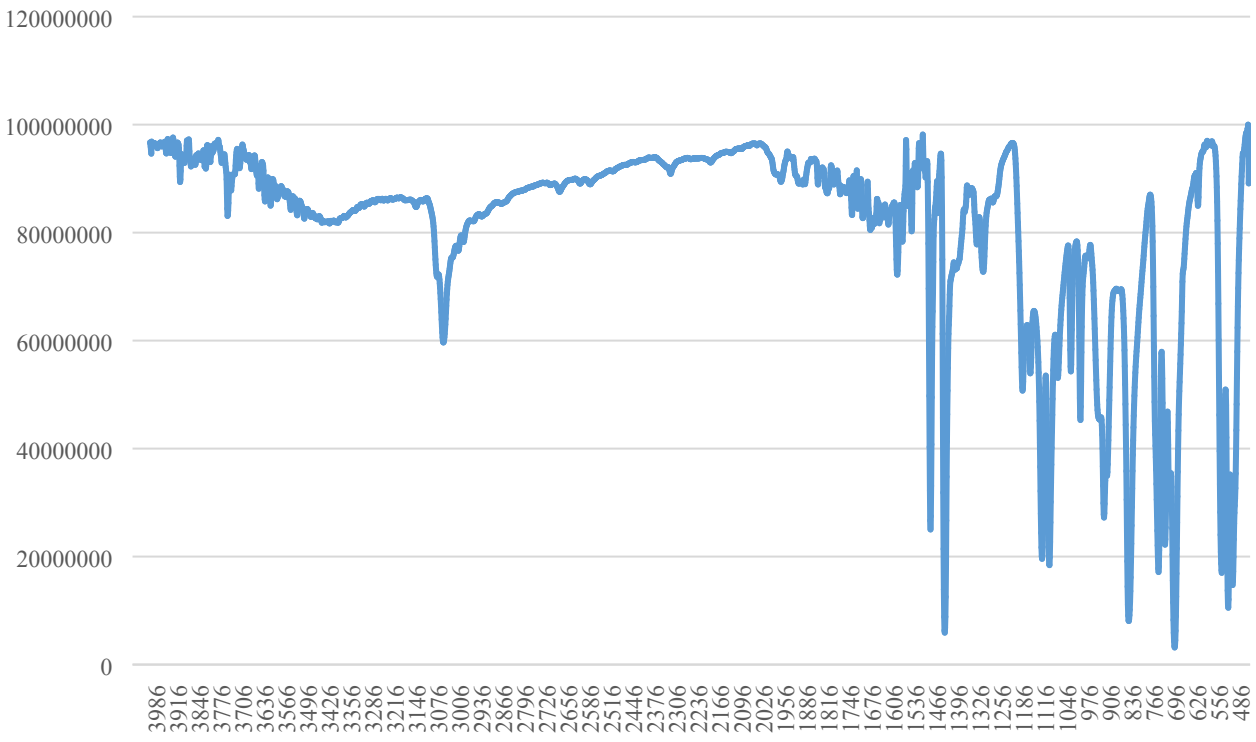

Figure S12. FT-IR spectrum of $ReO_2I[P(C_6H_5)_3]_2$ (**11**)

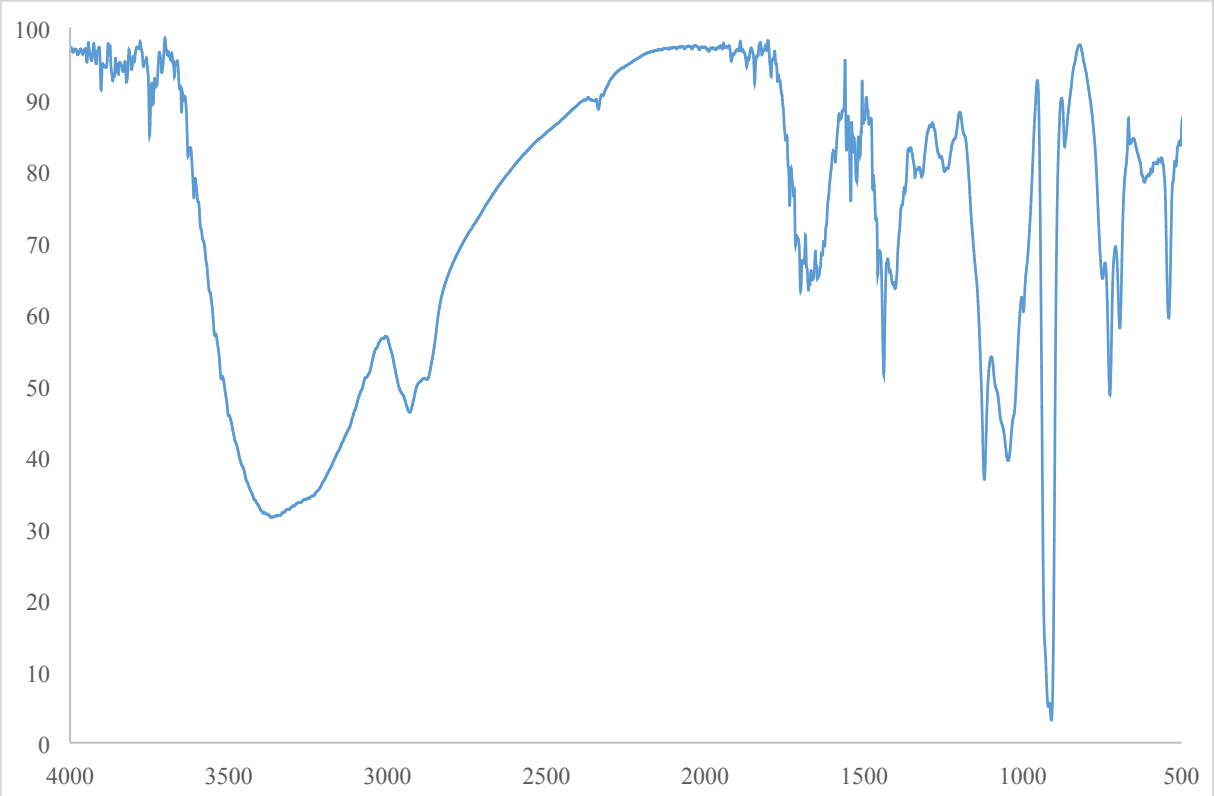

Figure S13. FT-IR spectrum of $ReO_2I[P(C_6H_5)_3]_2$ (**11**) after the delay time.

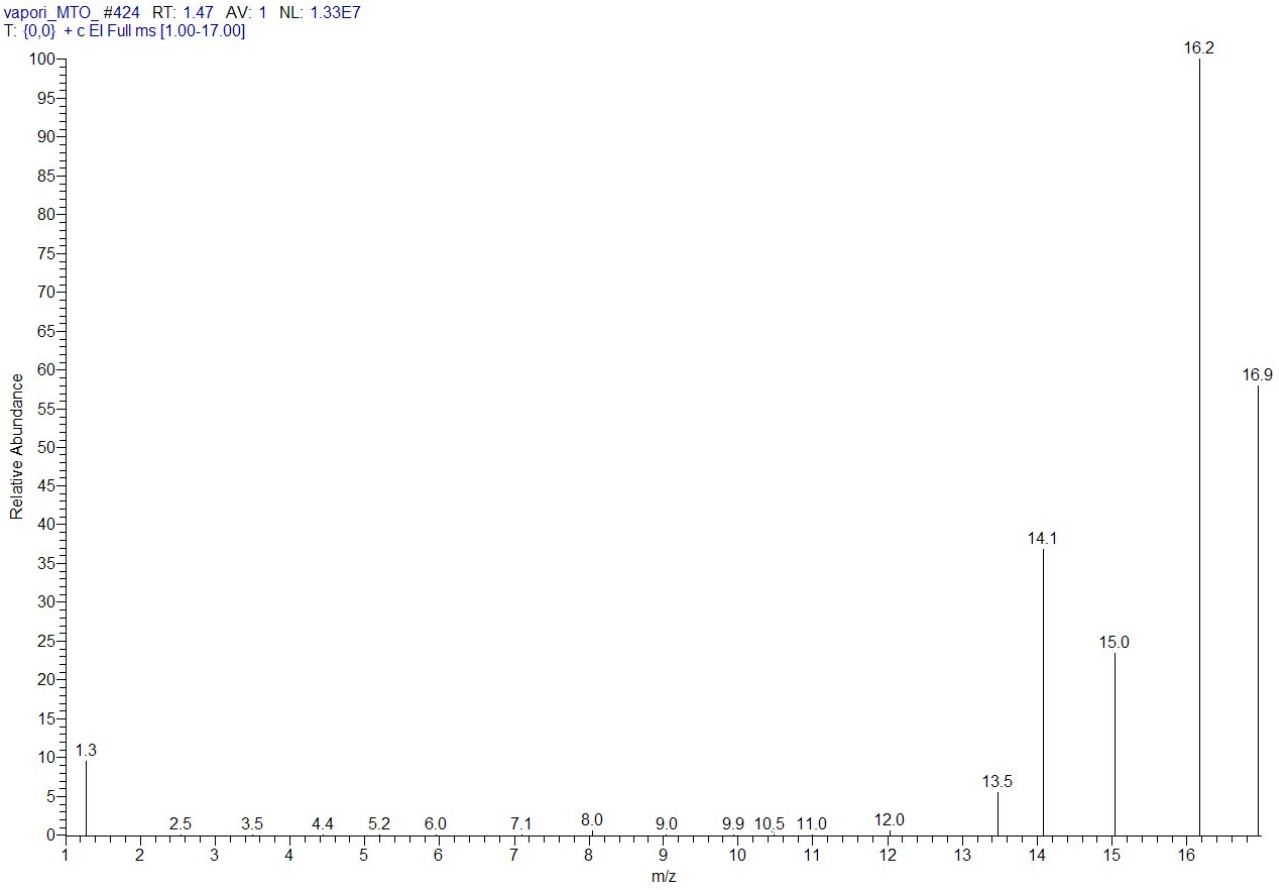

Figure S14. The mass spectrum of monodeuterated methane recorded by sampling the headspace of the reaction medium containing monodeuterated DMP (-OD) and MTO, and after a time comprised in the range of the detected delay time (MTO + DMP at 140 °C).

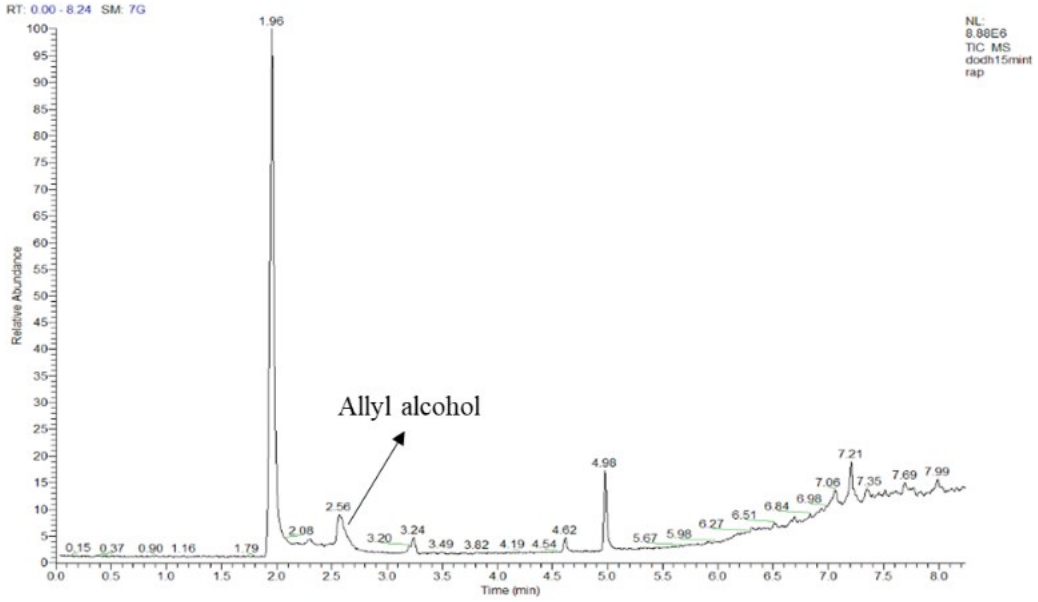

Figure S15. GC-MS profile of water trap headspace recorded after 10 min from the addition of glycerol. The catalyst (MTO) used in the present experiment was pretreated at 140C° in presence of only DMP for the delay time previously established (45 min). It is worth noting the almost immediate appearance of the chromatographic peak of allyl alcohol.

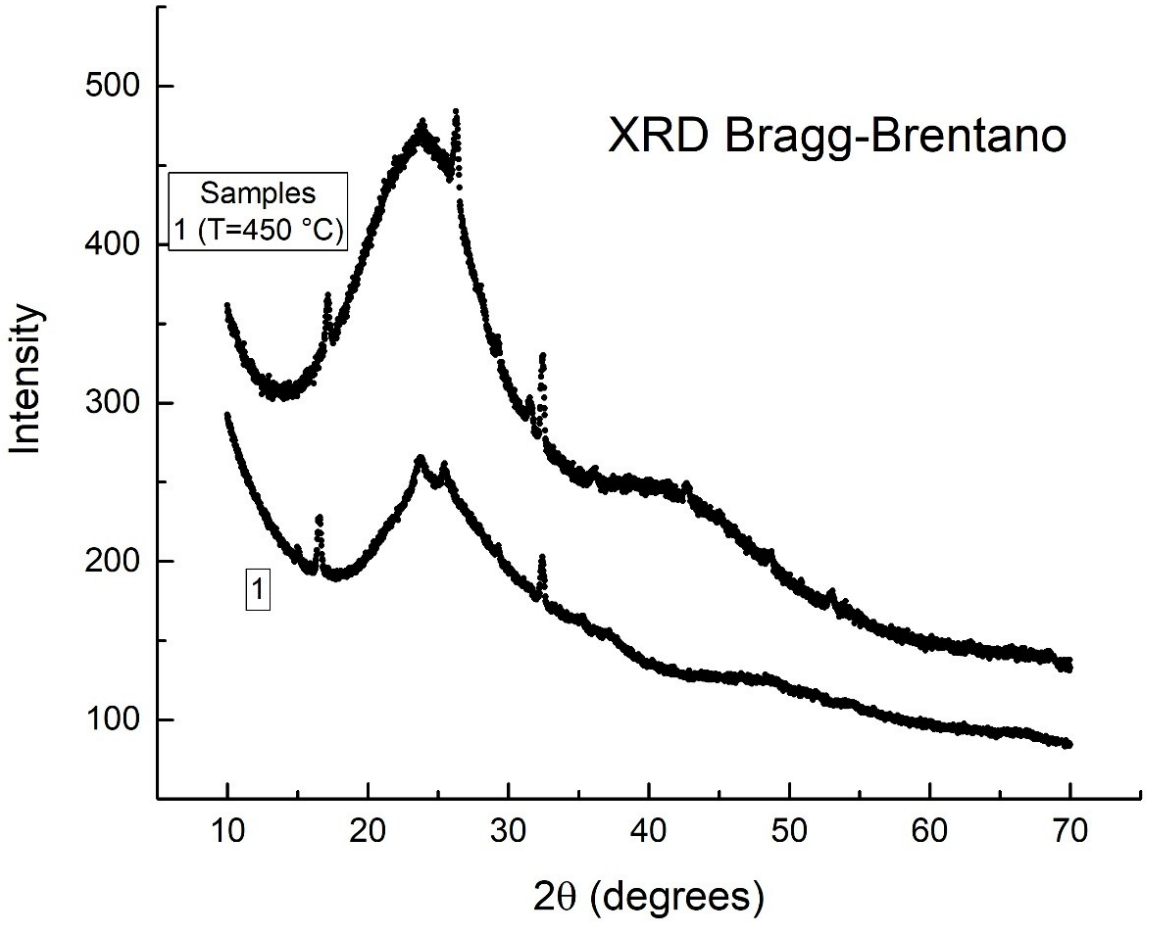

Figure S16. X-ray diffraction (XRD) of **1**, on samples treated at 140 °C and 450 °C.

(Bruker D5000 diffractometer with Cu K_α, λ = 1.5406Å) operating in the Bragg–Brentano mode (0.6 mm/Ni filter/0.2 mm (after the sample) were used in order to remove K_β radiation as well as to improve the resolution).

From the measurements carried out on **1** (with different annealing temperature), both samples are amorphous, however by superimposing the peak on the amorphous XRD spectra, it is evident a beginning of crystallization in the oxidized species of rhenium.

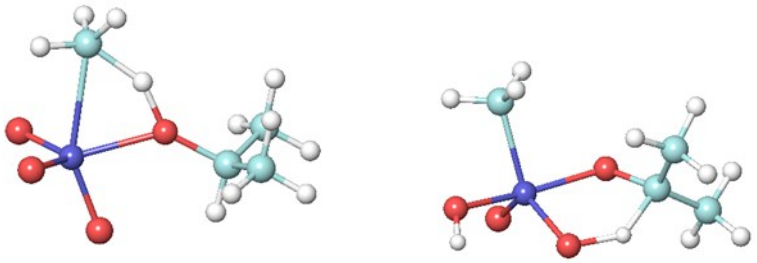

Figure S17. Ball-and-sticks representations of the calculated transition state structures for the methane release process (left) and MTO reduction (right).

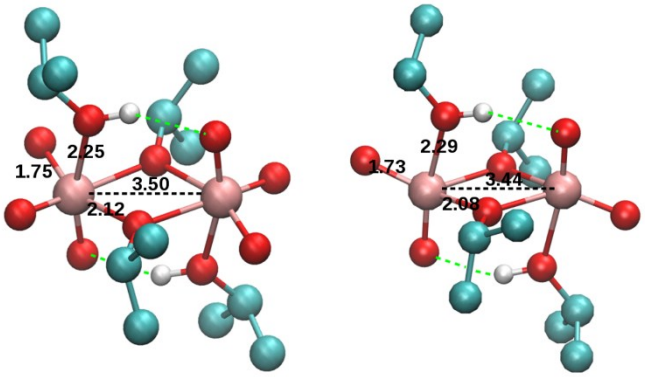

Figure S18. Ball-and-sticks representation of the optimized structure of $[ReO_3(2\text{-PrO})\cdot 2\text{-PrOH}]_2$ (right) and $[ReO_2(2\text{-PrO})\cdot 2\text{-PrOH}]_2$ (left). For sake of clarity, non-polar hydrogen are not displayed. Dashed lines indicate Re-Re distance (black) and hydrogen bond contacts (green). Bond distances in Angstrom.

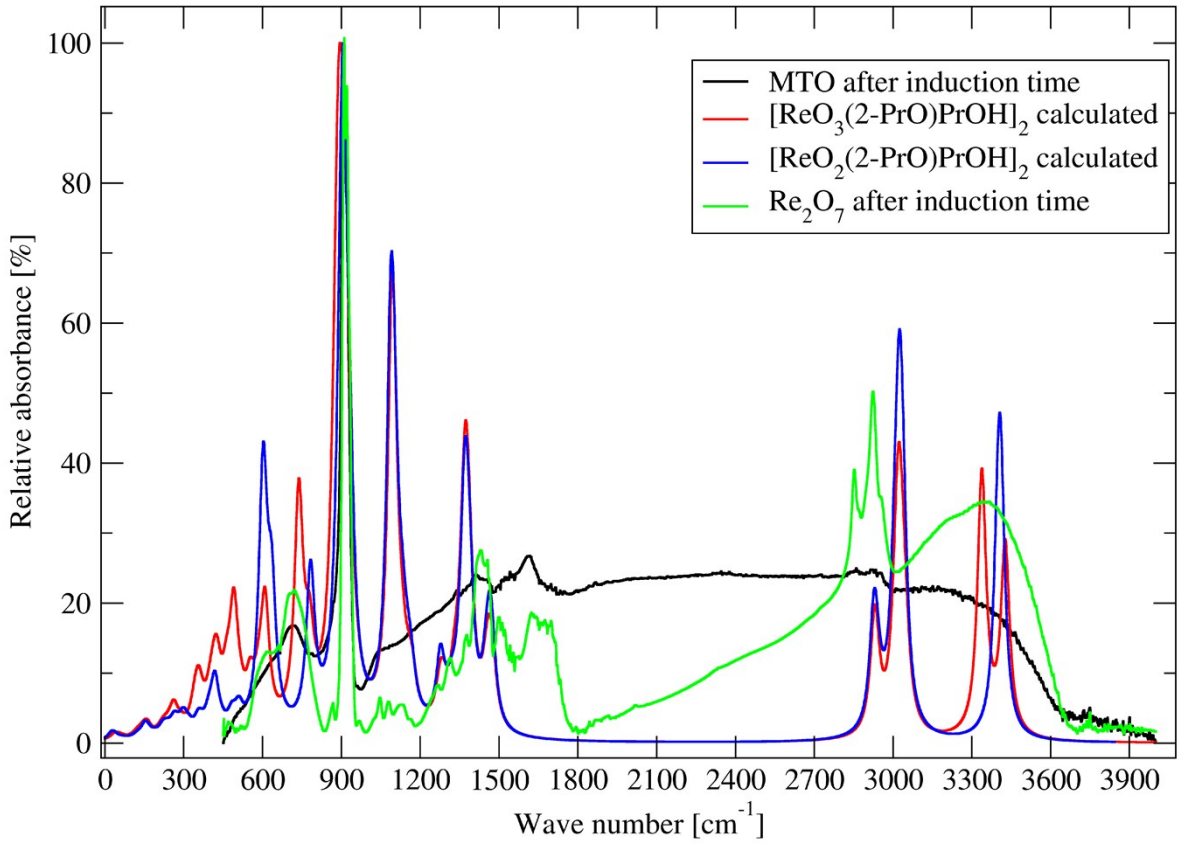

Fig. S19. Comparison between the experimental IR spectra of MTO and Re_2O_7 precipitate after the delay time and the theoretical IR spectra of $[ReO_3(2PrO)\cdot 2PrOH]_2$ and $[ReO_2(2\text{-}PrO)\cdot 2\text{-}PrOH]_2$.

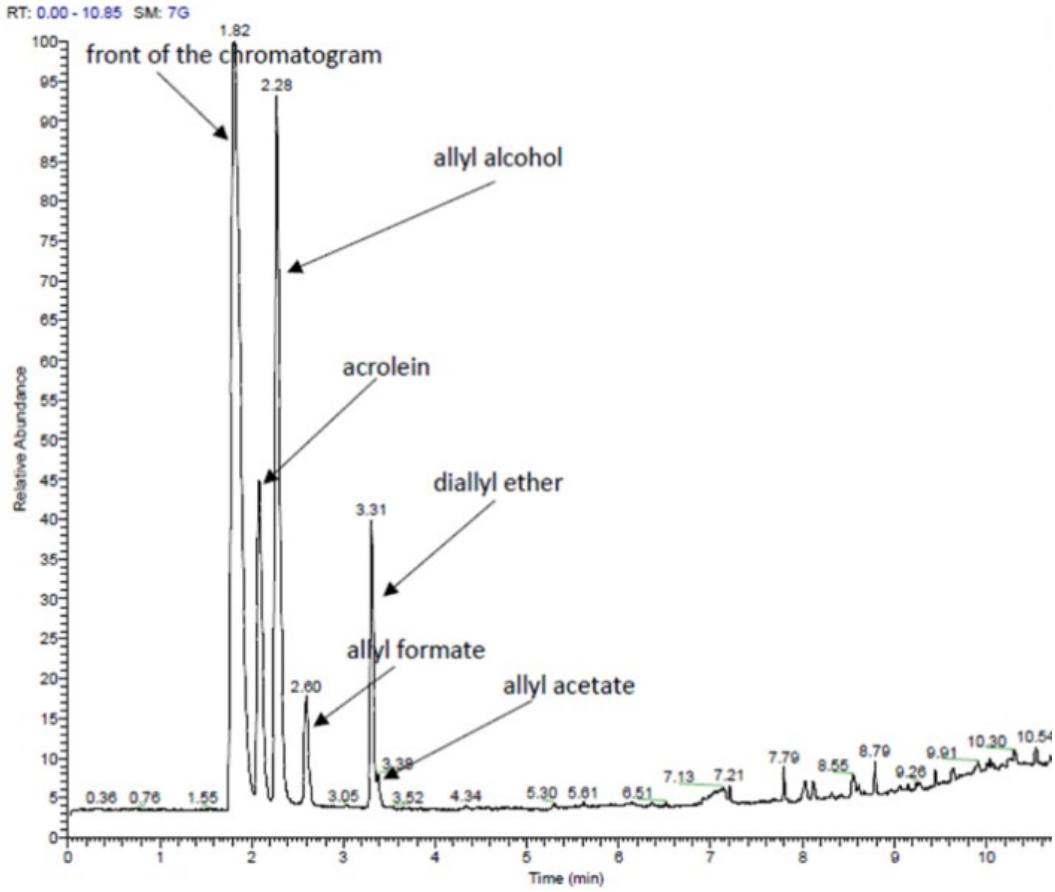

Figure S20. GC-MS chromatogram recorded during the course of DODH in presence of ReO_3, in aerobic conditions and in neat glycerol. Note that the chromatographic response factors of the various by-products like acrolein, allyl formate, diallyl ester, and allyl acetate are noticeably higher than that of allyl alcohol. Maximum molar concentrations of the whole content of the three secondary allyl derivatives (ether + acetate + formate) ranges around 5%

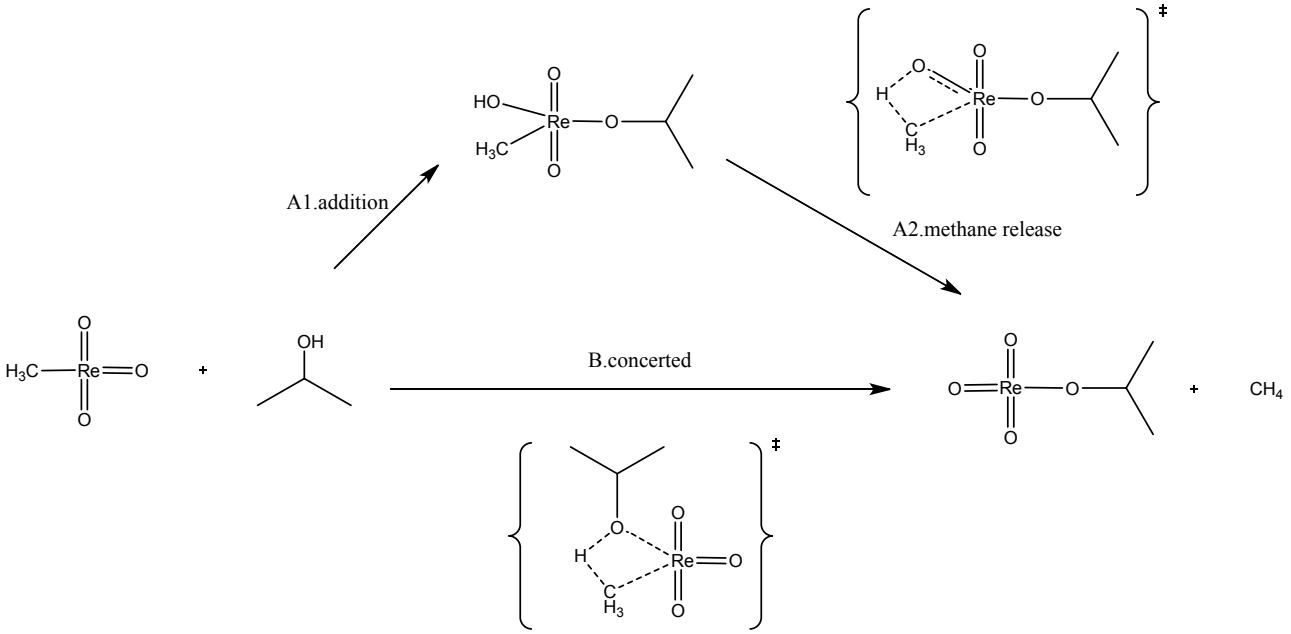

Scheme S1. Hypothesized solvent-assisted processes affording methane from MTO: A) two-step, and B) one-step (concerted) mechanism.

Table S1. Comparison between the experimental IR spectra of **1** and **5** after delay time and the theoretical IR spectra of $[ReO_3(2\text{-}PrO)\cdot PrOH]_2$ and $[ReO_2(2\text{-}PrO)\cdot PrOH]_2$ in the gas phase.

1	5	$[ReO_3(2\text{-}PrO)\cdot PrOH]_2$		$[ReO_2(2\text{-}PrO)\cdot PrOH]_2$	
ν (cm^{-1}) [a]	ν (cm^{-1}) [a]	ν (cm^{-1}) [a]	assignment	ν (cm^{-1}) [a]	assignment
Experimental values		Theoretical values			
716 b	609 b 716 b	609 738	$\nu(Re_2O_2)$ $\nu(Re_2O_2)$	635 784 604	$\nu(Re_2O_2)$ $\nu(Re_2O_2)$ τ (OH) [b]
919 n	910 n 921 n	890 910	$\nu(Re_2{=}O_2)_{asym}$ $\nu(Re_2{=}O_2)_{sym}$	932 906 898	$\nu(Re_2{=}O_2)_{asym}$ $\nu(Re_2{=}O_2)_{sym}$ $\nu(C\text{-}O)_{coupl.}$
1039 w	1050-1125 vw	1094 1096	ν(C-Oμ) [c] ν(C-O)	1088 1101	ν(C-O) ν(C-Oμ)
1340-1620 bm	1314 bm 1431 bm 1655 bm	1276 1456	δ(COH) $\delta_{(COH+CCH)}$ δ(CCH)	1276 1366 1467	δ(COH) $\delta_{(COH+CCH)}$ δ(CCH)
1620-3200 bm	2855 n 2927 n 3356 b	2934 3018 3339 3427	$\nu(C\text{-}H)_{sym}$ $\nu(C\text{-}H)_{asym}$ ν(O-H) ν(O-H)	2934 3025 3399 3410	$\nu(C\text{-}H)_{sym}$ $\nu(C\text{-}H)_{asym}$ ν(O-H) ν(O-H)

[a] Legend on frequences: b=broad, n=narrow, w=weak, m=multiplet, v=very

[b] Out-of-plane bending of O-H bond

[c] "Oμ" stands for bridged oxygen

Table S2. % Yields of acrolein in reactions conducted under air and hydrogen at 140 °C, in DMP; the reaction was stopped when allyl alcohol finished to be formed.

Catalyst	Yield (%)	
	Air	H_2
1	2.1	1.3
2	0.8	not detectable
4	0.4	0.9
5	2.4	2.6
7	1.4	0.9
9	0.9	1.1
10	2.8	2.4
11	2.5	2.1

Table S3. Oxygen to Rhenium ratio, determined gravimetrically simply recovering the residue of each Re compound, after 8 hours of treatment at 140 °C and subsequently after a treatment at 450 °C

Entry	Re compound	Mol. weight of Re deriv.	mg of initial Re derivative used	mmol. of initial Re derivative used	mg of Re (as free metal)	Sample after 450 °C treatment (mg)	mg of Oxygen in the residue	mmol of Oxygen in the residue	**O / Re** molar ratio
1	MTO	249.21	**50**	0.2	37.4	**46.6**	9.2	0.5775	**2.88**
2	ReO_3	234.31	**47**	0.2	37.4	**46.4**	9.0	0.5656	**2.82**
4	$ReCl_5$	263.46	**73**	0.2	37.4	**47.1**	9.7	0.6063	**3.02**
5	Re_2O_7	484.41	**48**	0.1	36.9	**44.7**	7.8	0.4874	**2.46**
7	ReI_3	566.92	**113**	0.2	37.1	**45.9**	8.8	0.5490	**2.75**
11	$ReO_2I(PPh_3)_2$	869.68	**174**	0.2	37.3	**45.8**	8.5	0.5341	**2.67**

Table S4. Rhenium content by ICP AES of samples recovered after a treatment of 8 hours at 140 °C

Entry	Re compound	mg of initial Re derivative used	mg of residue, after treatment at 140 °C	% of organic fraction inside the residue *	mg of Re oxide inside the residue	mg of Re (as free metal) inside the calcinated residue (from ICP AES)	% of Re inside the residue
1	MTO	**50**	127	61.17	49.3	39.8	**80.71**
2	ReO_3	**48**	109	55.81	48.2	38.8	**80.59**
4	$ReCl_5$	**73**	136	65.11	47.5	39.3	**82.84**
5	Re_2O_7	**50**	88	47.41	46.3	36.7	**79.30**
7	ReI_3	**115**	143	63.28	52.5	42.4	**80.75**
11	$ReO_2I(PPh_3)_2$	**175**	315	85.69	45.1	38.8	**86.08**

* data listed in this column were obtained from the samples treated at 450 °C and listed in **Table S3**

Table S5. Cartesian coordinates (in Angstrom) of transition state structures.

path A, TS reduction: imaginary frequency -1349.7 cm^{-1}			
atom	**x**	**y**	**z**
C	2.516522	1.379041	-0.489365
C	2.144049	-0.042644	-0.071147
C	3.274933	-1.035729	0.096719
O	1.020567	-0.586718	-0.706204
Re	-0.767410	-0.338317	-0.083794
O	-2.284969	0.704686	0.533645
O	-1.360023	-1.949709	0.024374
O	0.180419	0.324914	1.368410
H	1.414470	0.188618	1.066832
H	3.211602	1.807966	0.240349
H	3.020085	1.360477	-1.466145
H	1.635450	2.025452	-0.561693
H	3.991045	-0.665307	0.839164
H	2.897208	-2.011463	0.418372
H	3.817043	-1.166196	-0.851348
H	-2.237971	1.093888	1.432387
C	-1.370030	0.473442	-1.945667
H	-2.463252	0.500359	-1.968360
H	-0.983291	1.498575	-2.019251
H	-0.955914	-0.140045	-2.753378

path B, TS CH4 release: imaginary frequency -1515.7 cm^{-1}			
atom	**x**	**y**	**z**
C	-0.404869	2.305635	-0.088962
Re	-0.684044	-0.114859	0.345500
O	-0.219308	-1.779201	0.115215
O	1.226796	0.390241	-0.138454
C	2.552918	-0.295742	-0.258550
C	3.500168	0.717307	-0.909089
O	-2.225506	0.086543	-0.438350
O	-0.927979	0.112086	2.044788
C	3.007382	-0.765381	1.126742
H	0.726653	1.496503	-0.156429
H	3.980482	-1.265322	1.041676
H	3.114780	0.086904	1.808374
H	2.293902	-1.477299	1.555409
H	4.479245	0.249962	-1.070806
H	3.112578	1.052189	-1.877571
H	3.638571	1.590035	-0.259303
H	0.368067	3.070429	0.114300
H	-0.828509	2.464542	-1.082199
H	-1.168162	2.472808	0.678302
H	2.382344	-1.151319	-0.920903

path B, TS reduction: imaginary frequency -1238.9 cm^{-1}			
atom	**x**	**y**	**z**
C	3.168202	-1.009912	0.196358
C	2.178303	0.062652	-0.199622
C	2.701661	1.409519	-0.642226

O	1.067475	-0.401582	-0.929248
Re	-0.689559	-0.613832	-0.286126
O	-1.183116	-2.251010	0.049989
O	-1.858936	0.522065	-0.905512
O	0.126244	0.087072	1.214287
H	1.281772	0.270298	0.958191
H	3.361144	1.825046	0.127771
H	3.297108	1.300129	-1.561410
H	1.884627	2.110577	-0.838611
H	3.833017	-0.633357	0.981431
H	2.660843	-1.912334	0.551527
H	3.796175	-1.279132	-0.666490

path B, TS DODH: imaginary frequency -395.3 cm^{-1}			
atom	**x**	**y**	**z**
C	1.923417	-1.282519	0.936844
C	2.365844	-0.927671	-0.362105
C	3.262714	0.279360	-0.593968
O	3.013526	1.363519	0.346412
H	2.455726	-1.711209	-1.113650
H	1.713440	-2.322009	1.168069
H	2.200731	-0.646564	1.771856
H	4.309962	-0.000838	-0.426905
H	3.155198	0.617571	-1.634376
H	2.163112	1.808240	0.143870
O	0.044503	-0.804312	1.093909
Re	-0.710357	0.039460	-0.294096
O	0.780585	-0.179183	-1.265038
O	-2.210124	-0.806845	-0.981356
H	-2.642981	-1.613217	-1.301010
O	-0.877007	1.711215	0.096274

dimer-eta1 TS reduction: img frequency -1282.5 cm^{-1}			
atom	**x**	**y**	**z**
C	4.397169	-1.458817	0.910250
C	3.710801	-0.097528	1.096251
C	3.812096	0.438315	2.526672
O	2.262278	-0.223605	0.790321
Re	1.456809	-0.218097	-0.952632
O	0.072129	-0.111119	-2.231890
O	-0.108840	-1.088642	0.208743
C	0.097360	-2.486398	0.737253
C	-0.372850	-3.480709	-0.333480
O	0.222279	1.341841	0.007925
C	0.372621	2.820311	-0.175009
C	1.706186	3.290608	0.419790
O	2.132368	-1.727763	-1.474473
O	2.552348	0.955634	-1.606997
Re	-1.494462	0.430425	0.791275
O	-2.307409	-0.089374	-0.949555
C	-3.597800	-0.605991	-0.994510
C	-4.717678	0.426124	-0.970473
O	-2.252598	1.972743	0.873598
O	-2.855744	-0.665840	1.370840
O	-0.596599	0.336742	2.496205

C	-0.576190	-2.722331	2.093501
C	0.191743	3.198875	-1.652139
C	-3.778122	-1.814438	-1.889144
H	-0.904424	-0.145402	-2.041660
H	1.183278	-2.560385	0.866739
H	-0.451688	3.248356	0.405572
H	0.345369	0.622814	2.465471
H	-3.507934	-0.982099	0.404210
H	4.121480	0.630130	0.378047
H	5.477881	-1.349022	1.070608
H	4.010996	-2.185183	1.635805
H	4.238031	-1.853956	-0.098593
H	3.315012	1.410563	2.614550
H	3.343618	-0.261799	3.228769
H	4.865896	0.561291	2.809973
H	-4.702291	-2.346201	-1.632797
H	-3.860074	-1.501633	-2.942354
H	-2.930690	-2.500459	-1.804468
H	-4.524384	1.206595	-0.227334
H	-4.801045	0.908561	-1.956945
H	-5.677330	-0.055280	-0.749535
H	-0.268137	-3.714532	2.451931
H	-0.279778	-1.970277	2.827458
H	-1.667339	-2.704291	2.016430
H	0.099191	-3.278505	-1.299908
H	-0.101017	-4.499606	-0.026046
H	-1.462869	-3.439728	-0.443194
H	0.220249	4.292939	-1.747445
H	0.986392	2.776367	-2.275002
H	-0.775704	2.847835	-2.027744
H	1.793664	2.980257	1.467631
H	2.556867	2.897200	-0.144930
H	1.747014	4.387828	0.384965

dimer-mu TS reduction: img frequency -396.5 cm^{-1}			
atom	**x**	**y**	**z**
C	4.448549	-0.408456	1.896871
C	3.817816	0.334353	0.712389
C	4.034744	1.851917	0.746936
O	2.363152	0.022307	0.675011
Re	1.112826	-0.435741	-1.204012
O	-0.182681	-0.758776	-2.339548
O	0.157619	-1.288165	0.383936
C	0.194998	-2.616546	0.770423
C	-0.689254	-3.549126	-0.020616
O	0.074596	1.227869	-0.434483
C	0.191303	2.646783	-0.914660
C	-1.030605	3.002777	-1.770577
O	1.965399	-2.109591	-1.193444
O	2.367017	0.544597	-1.947983
Re	-1.142355	0.448391	1.175651
O	-2.239538	-0.159691	-0.658042
C	-3.723389	-0.191085	-0.828930
C	-4.061262	0.280759	-2.247822
O	-2.137299	1.871872	1.209098

O	-2.084107	-0.768313	1.989034
O	0.171839	0.785224	2.281076
C	0.456828	-2.882569	2.227645
C	0.416447	3.604028	0.261221
C	-4.248602	-1.592493	-0.496668
H	-1.710030	-0.427505	-1.457302
H	1.673425	-2.688279	-0.371683
H	1.088175	2.615929	-1.546095
H	1.852196	0.343701	1.458159
H	-4.078850	0.534949	-0.091016
H	4.178259	-0.072372	-0.235614
H	5.536371	-0.263051	1.893846
H	4.060214	-0.032949	2.853639
H	4.243680	-1.482723	1.830180
H	3.555068	2.321776	-0.117089
H	3.631604	2.290642	1.670206
H	5.108752	2.074763	0.707865
H	-5.346094	-1.592622	-0.527872
H	-3.885130	-2.330377	-1.223523
H	-3.929507	-1.887634	0.507730
H	-3.661067	1.282971	-2.433809
H	-3.653992	-0.407626	-3.000411
H	-5.150190	0.313635	-2.376181
H	0.791149	-3.917697	2.369136
H	1.214411	-2.201061	2.627168
H	-0.465396	-2.746789	2.819325
H	-0.624624	-3.345914	-1.097333
H	-0.413398	-4.592780	0.168917
H	-1.743453	-3.421736	0.281937
H	0.654327	4.602259	-0.131331
H	-0.477017	3.685695	0.888404
H	1.254288	3.272328	0.883105
H	-1.146925	2.289640	-2.594516
H	-1.941600	3.009016	-1.162618
H	-0.893397	4.004375	-2.200595